

REPORT DOCUMENTATION PAGE		READ INSTRUCTIONS BEFORE COMPLETING FORM
1. REPORT NUMBER NRL Report 7760	2. GOVT ACCESSION NO.	3. RECIPIENT'S CATALOG NUMBER
4. TITLE (and Subtitle) GEOLOGIC AND GEOMAGNETIC BACKGROUND NOISE IN TWO AREAS OF THE NORTH ATLANTIC	5. TYPE OF REPORT & PERIOD COVERED Final report on one phase of a continuing problem.	
	6. PERFORMING ORG. REPORT NUMBER	
7. AUTHOR(s) Perry B. Alers John M. Bergin	8. CONTRACT OR GRANT NUMBER(s)	
9. PERFORMING ORGANIZATION NAME AND ADDRESS Naval Research Laboratory Washington, D.C. 20375	10. PROGRAM ELEMENT, PROJECT, TASK AREA & WORK UNIT NUMBERS NRL Problem G03-01 RR 131-03-41-5905	
11. CONTROLLING OFFICE NAME AND ADDRESS Department of the Navy Office of Naval Research Arlington, Va. 22217	12. REPORT DATE July 25, 1974	
	13. NUMBER OF PAGES 24	
14. MONITORING AGENCY NAME & ADDRESS (if different from Controlling Office)	15. SECURITY CLASS. (of this report) Unclassified	
	15a. DECLASSIFICATION/DOWNGRADING SCHEDULE	
16. DISTRIBUTION STATEMENT (of this Report) Approved for public release; distribution unlimited.		
17. DISTRIBUTION STATEMENT (of the abstract entered in Block 20, if different from Report)		
18. SUPPLEMENTARY NOTES		
19. KEY WORDS (Continue on reverse side if necessary and identify by block number) Quiet Zone Seamounts geomagnetic noise micropulsations paleomagnetism		
20. ABSTRACT (Continue on reverse side if necessary and identify by block number) Surface magnetic fields were measured in two areas of the North Atlantic Quiet Zone in order to characterize the level of magnetic interference arising from geological features in the sea floor. One area included several of the New England seamounts, and we find that they are isolated in their magnetic effects; the surrounding magnetic environment is not significantly different from that found elsewhere in the Quiet Zone. In the other area a sufficient number of tracks was followed to reveal the presence of low-amplitude magnetic features in which a N-NE trend can be discerned and whose wavelength, 30-40 km, is comparable to that found in more active areas to (over)		

(20 continued)

the east. A filtering technique used on the data enabled us to separate geologic from geomagnetic noise, and the difference between interference encountered on quiet and noisy days is quantitatively described.

CONTENTS

INTRODUCTION	1
METHODS OF MEASUREMENT	1
DATA TREATMENT	2
RESULTS AND DISCUSSION	3
Geological Contributions	3
Geomagnetic Noise	18
CONCLUSIONS	20
SUGGESTIONS FOR FUTURE WORK	20
ACKNOWLEDGMENTS	21
REFERENCES	21

GEOLOGIC AND GEOMAGNETIC BACKGROUND NOISE IN TWO AREAS OF THE NORTH ATLANTIC

INTRODUCTION

The effectiveness of magnetic detection devices used at sea is limited by three major sources of external noise. Two are time-dependent and are due to wave action and geomagnetic (ionospheric) fluctuations. The third reflects the magnetic geology of the seabed and occupies a position in the noise spectrum that is a function of the speed at which the detector passes over the magnetic formations. The measurements described in this report were made in the so-called Quiet Zone of the North Atlantic. This zone is a band that runs parallel to the continental shelf of North America and extends at least 20 mi to the east of it. It is notable because of the absence of any strong spatial magnetic features, a characteristic that contrasts sharply with the increase in amplitude of anomalies which sets in toward the Mid-Atlantic Ridge.

Our primary purpose was to make surface magnetic measurements in two areas of the Quiet Zone to determine the size of the magnetic anomalies that could be attributed to bottom geology. In addition, one area was chosen to include several of the seamounts in the New England Seamount Chain, so that we could see what effect, if any, the presence of these features had on the surrounding magnetic terrain. Finally, while the data were being gathered, we encountered several days of moderately high magnetic activity. We have extracted these noise components from the magnetic records and determined the number and size of the pulsations to characterize this source of interference, especially as it is observed at sea.

METHODS OF MEASUREMENT

The cruise (NRL No. 73-11-05) was made aboard the USNS *Mizar* (T-AGOR 11) from May 24, 1973, to June 15, 1973. Measurements were made in two areas, one bounded by 40° N, 60° W, 38° N, and 64° W, the Seamounts area, and the other bounded by 36° N, 69° W, 34° N, and 73° W, the Blake area. A bathymetric chart showing the tracks followed is given in Fig. 1. Ship speed was usually 7 to 8 knots.

The magnetic data were taken with a Geometrics G-803 Marine Magnetometer of the proton resonance type with an internal noise level of the order of 0.2 γ . The sensor head was towed about 300 m behind the ship. Readings were taken at 10-s intervals and presented in both analog and digital form. The digital data, together with time and Julian date, were recorded on magnetic tape by a Geometrics G-704 Data Acquisition System. Navigational fixes were taken from both a loran-C receiver at 30-min intervals and from a

satellite navigation system. The loran fixes were plotted on specially prepared charts and were used to determine true speed and heading to correct and update the parameters used by the computer in the satellite navigation receiver.

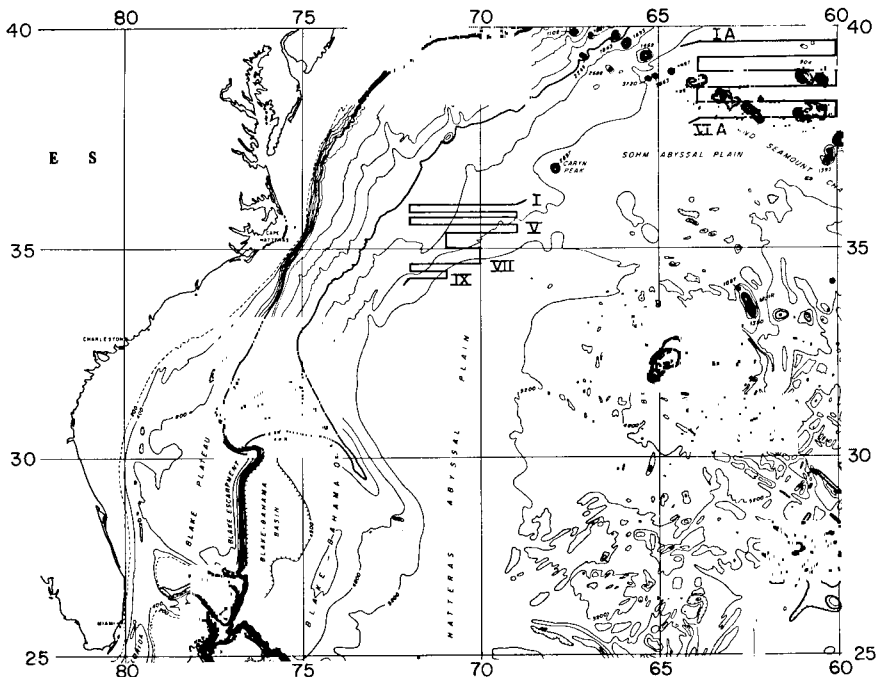


Fig. 1 — Bathymetric chart showing the tracks followed in this work. The Seamounts area is in the upper right corner, and the Blake area is near the center of the chart.

DATA TREATMENT

Upon our return to NRL, both the navigation and magnetic field data were fed into the CDC 3800 computer; the following routines were used to produce the results reported here.

The field and navigation readings were combined to produce graphs of field vs distance. In this form, the data could be used to construct a magnetic chart of the area if one were desired.

Given the position coordinates, the International Geomagnetic Reference Field (IGRF) at each point was calculated from an existing subroutine and subtracted from the measured field to yield a set of residual field values. These residual fields were used in all subsequent calculations.

A fast Fourier transform subroutine was then applied to the data for a given track. This produced the coefficients of the terms in the Fourier series that described the data analytically. The transform and filter processes are described in an earlier report [1].

The field values were filtered through a passband of given wavelength by discarding all terms in the series that fell outside the limits of the band. We used bands of 0.1 to 0.5, 0.5 to 5.0, and 5.0 to 50 km. At 8 knots these translate into periods of 24 to 120, 120 to 1200, and 1200 to 12,000 s, or 20 min to 3.3 hr.

Each set of filtered data was then sorted according to amplitude Γ and wavelength λ to obtain distribution histograms of the form $N(\Gamma)$ vs Γ and $N(\lambda)$ vs λ . These show the number of anomalies N that appear in a given range of values of Γ and λ . The height Γ of a given peak was taken to be the average of two heights measured from the associated minima on either side. The horizontal distance between the minima determined λ . Sorting was accomplished by counting the number of values of Γ or λ that fell between preset limits. Intervals of 1 γ or 1 km were used in the 1 to 10 γ or km range, and 20 γ or 20 km were used in the 10 to 100 range.

We found that the content of each band could be identified, for the most part, with one particular source of magnetic noise. The 24-to 120-s band contained instrument noise and possible contributions from long-period ocean waves; the 120-to 1200-s band contained most of the geomagnetic noise; and the third band, better expressed in terms of distance, 5 to 50 km, contained the geologic features. Surges of geomagnetic noise lasting longer than 20 min could also appear in this band, but the amplitude of such signals, identified from land-based observatory traces, tended to be much lower than the geological signatures of comparable wavelength. The effect of the diurnal variation, a 4- to 5-hr fluctuation that occurs around noon each day, was minimized by our choice of the long-wave cutoff of this filter; no further correction seemed necessary.

RESULTS AND DISCUSSION

Geological Contributions

The component of the surface field attributable to bottom geology arises not only from differences in elevation of the sea floor but also from variations in the magnetization of the floor itself. These variations reflect reversals in the earth's dipole field that appear to have taken place over the past 150 million years and are recorded in the magnetic material forced up through the earth's crust as part of the process of sea floor spreading. In the Quiet Zone, the magnetic subbottom is covered with a layer of sediment ranging from 0.5 to 1.0 km thick, and comparatively little is known about its configuration. Our traces, therefore, cannot be separated unambiguously into bottom topography and magnetization components. Nevertheless, the general magnetic characteristics of both the Seamounts and Blake areas appear to be similar, and there are correlations among the data taken in the Blake area that we tentatively ascribe to changes in magnetization.

Figure 2 shows the residual fields measured on the six tracks IA to VIA followed in the Seamounts; it is clear that very sharp gradients exist in the surface fields in their vicinity. These gradients have made it necessary for us to use only those portions of the tracks that do not contain individual seamount signatures when we filter the data prior to sorting; such gradients generate spurious wavelength components that extend throughout each record and produce false counts. The results of sorting according to both amplitude Γ and wavelength λ in the 5-to-50-km band are given in Figs. 3 and 4. The results for the truncated tracks have been appropriately scaled to allow valid comparisons to be made.

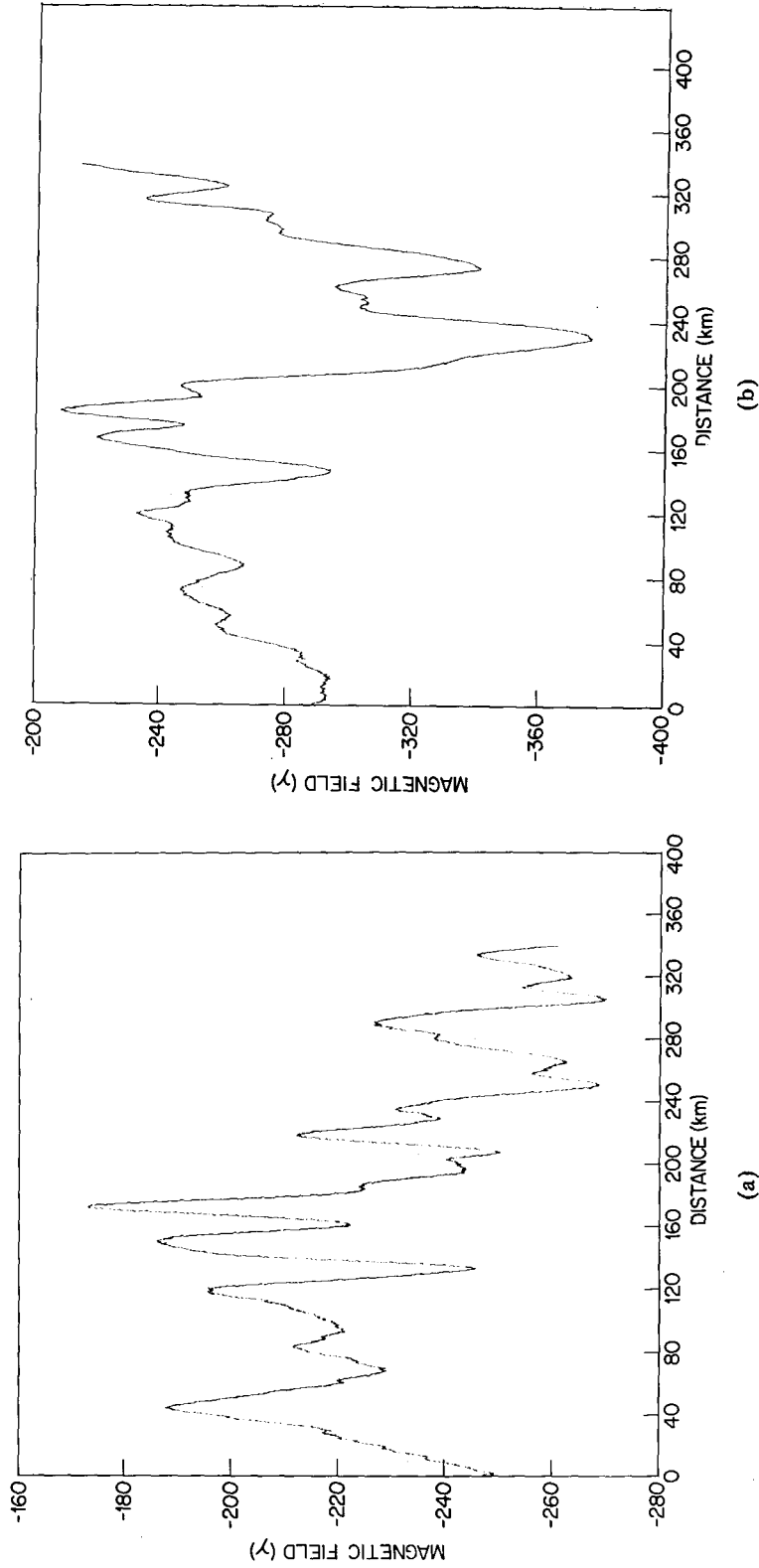


Fig. 2 -- Residual fields measured in the Seamounts area. All distances are measured from west to east, and all have the same scale. (a) Track IA, (b) Track II, (c) Track III, (d) Track IV; the peak at the west end is due to Kevin Seamount, and a contribution from San Pablo is visible at the east end. (e) Track VA; peaks from west to east are due to Atlantis II, Sheldrake, and the Manning group. (f) Track VIA; peak is due to Gosnold Seamount.

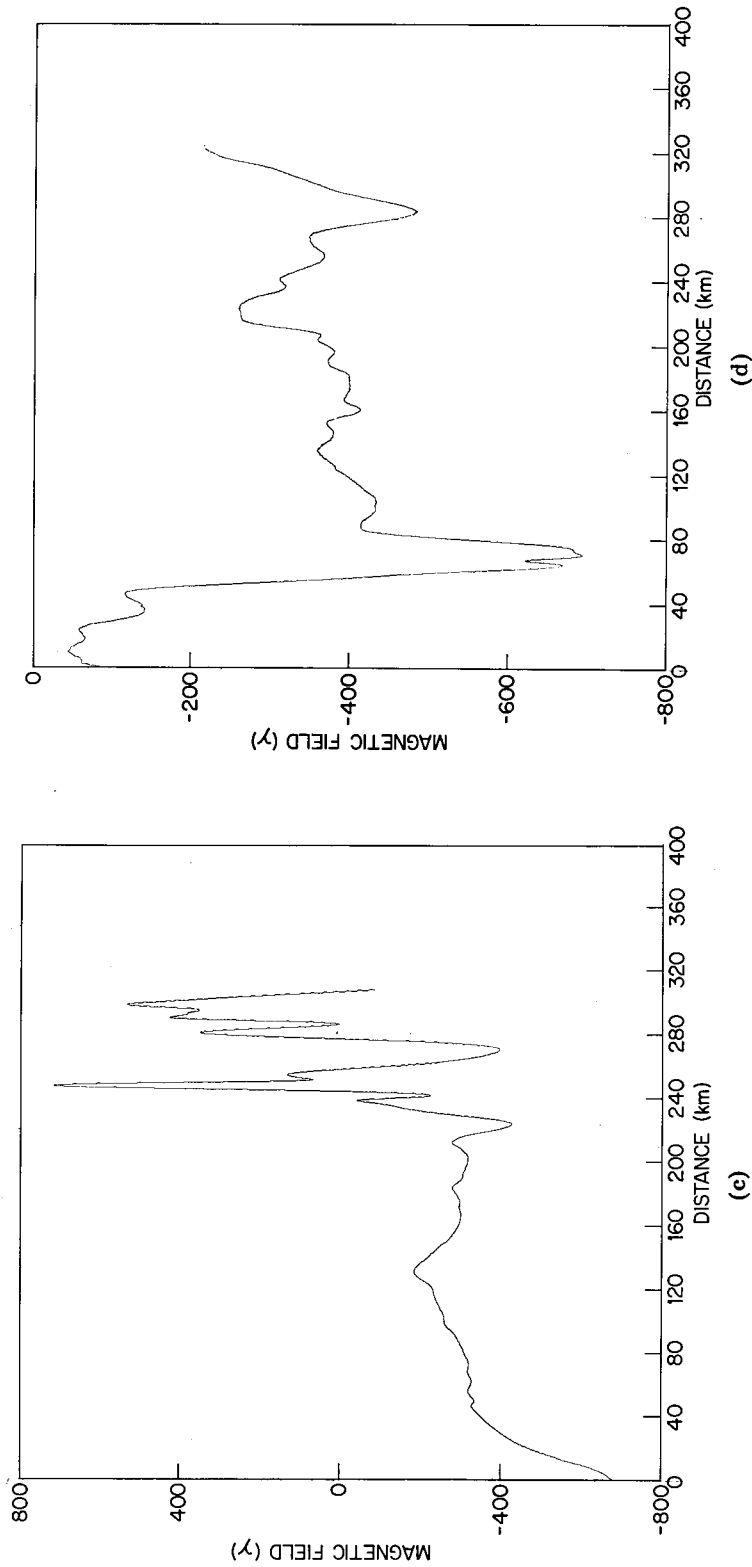


Fig. 2 (continued) — Residual fields measured in the Seamounts area. All distances are measured from west to east, and all have the same scale. (a) Track IA, (b) Track II, (c) Track IIIA; peaks at the east end are from Gregg and San Pablo Seamounts (d) Track IV; the peak at the west end is due to Kelvin Seamount, and a contribution from San Pablo is visible at the east end. (e) Track VA; peaks from west to east are due to Atlantis II, Sheldrake, and the Manning group. (f) Track VIA; peak is due to Gosnold Seamount.

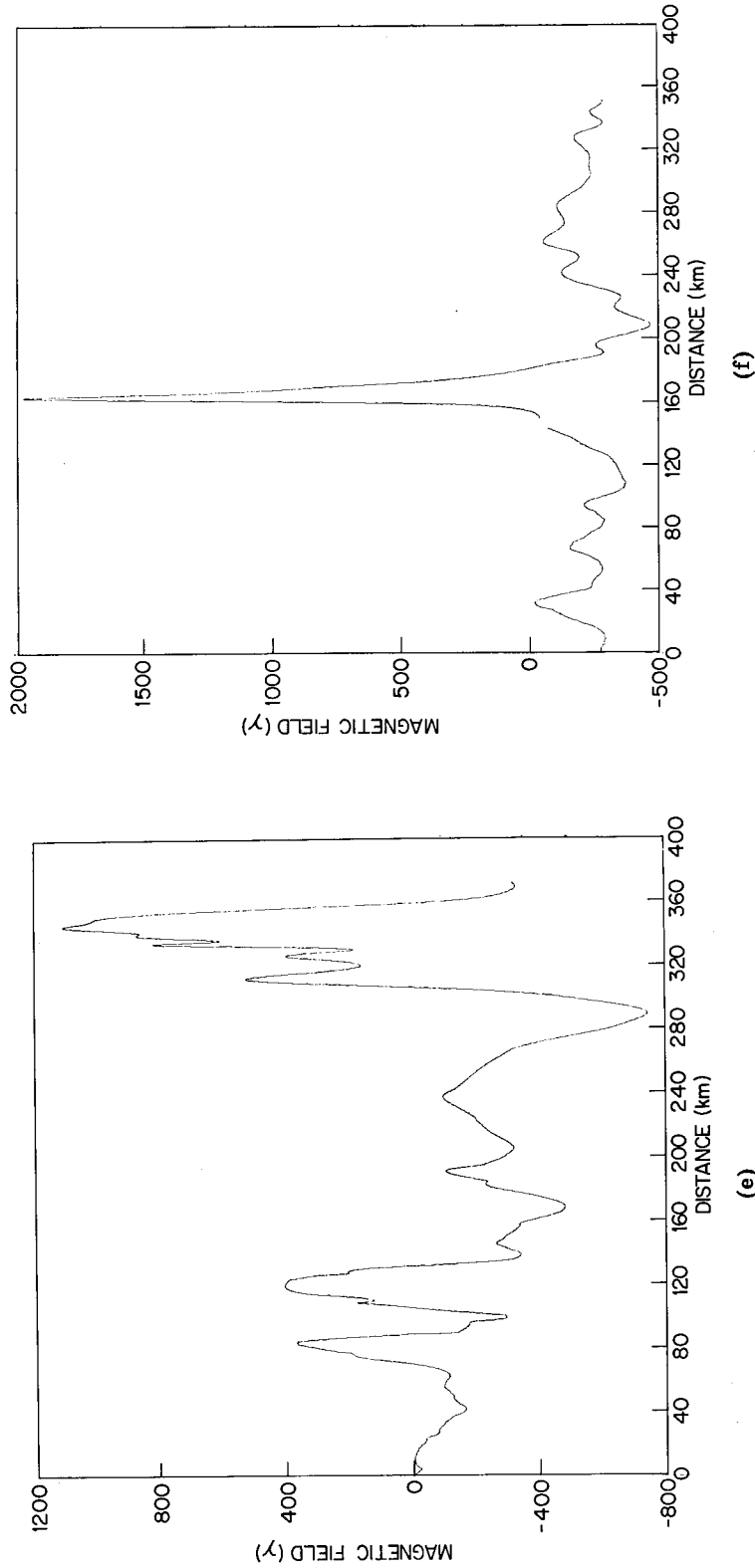


Fig. 2 (continued) — Residual fields measured in the Seamounts area. All distances are measured from west to east, and all have the same scale. (a) Track IA, (b) Track IIA, (c) Track IIIA, peaks at the east end are from Gregg and San Pablo Seamounts. (d) Track IV; the peak at the west end is due to Kelvin Seamount, and a contribution from San Pablo is visible at the east end. (e) Track VA; peaks from west to east are due to Atlantis II, Sheldrake, and the Manning group. (f) Track VIA; peak is due to Gosnold Seamount.

Track VA was not sorted at all because we were unable to isolate an undisturbed portion long enough to give reliable results. Comparison of the histograms for the abbreviated tracks with those for tracks IA and IIA show that they all have similar characteristics, an indication that the seamounts' effects are quite localized and affect their magnetic surroundings very little. This is consistent with their appearance in the acoustic profiles published by Uchupi, Phillips, and Prada [2], which show the mounts rising abruptly out of sediment-covered surroundings. Furthermore, the amplitude histograms for this area are similar to those shown in Fig. 8 for the Blake area, which suggests that both regions have similar magnetic geology.

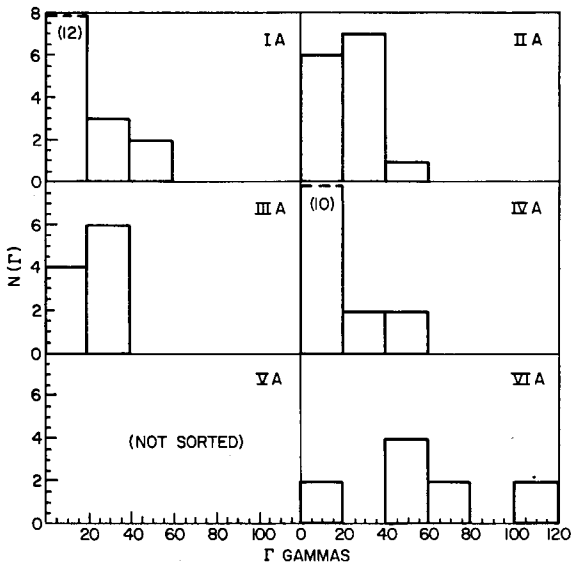


Fig. 3 — Amplitude histograms for the 5-to 50-km filter outputs, Seamount tracks. The seamount signatures themselves were removed before filtering and sorting took place; the counts have been appropriately scaled in compensation.

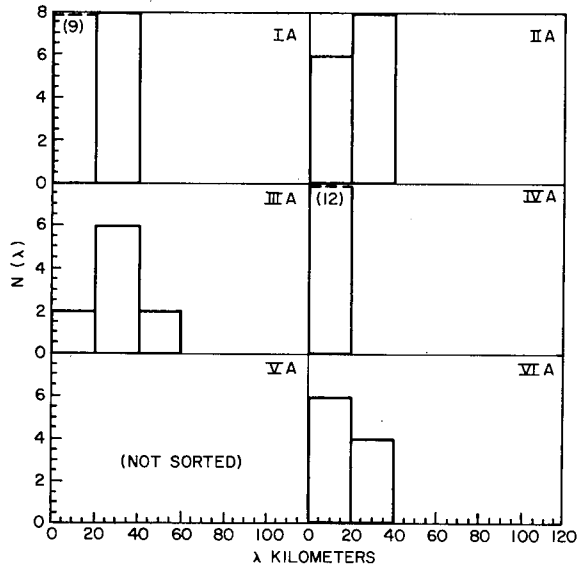


Fig. 4 — Wavelength histograms for the 5-to 50-km filter outputs, Seamount tracks. The seamount signatures themselves were removed before filtering and sorting took place; the counts have been appropriately scaled in compensation.

The data for tracks I to IX in the Blake area are given as residual fields as a function of distance in Fig. 5. As before, these data were filtered, and the geological components contained in the 5-to 50-km band were passed through the sorting routines. However, records for tracks VI, VIII, and IX all contained substantial amounts of geomagnetic noise as well, and the change in the output of the medium-wave (120 to 1200 s) filter for these records was significant. To show this and to illustrate the filtering process, we present in Figs. 6 and 7 the residual fields and their associated filtered components for both tracks V (quiet) and VII (noisy).

ALERS AND BERGIN

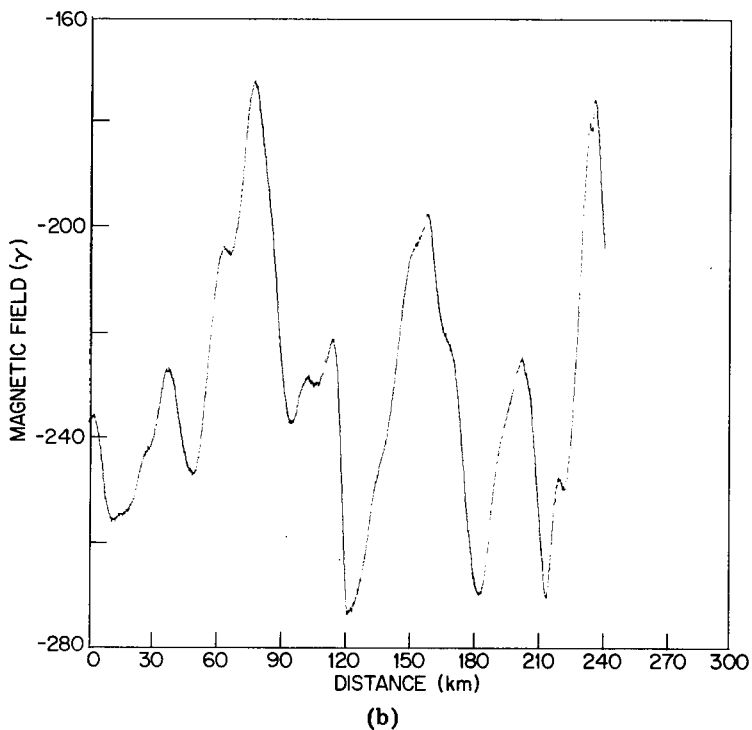
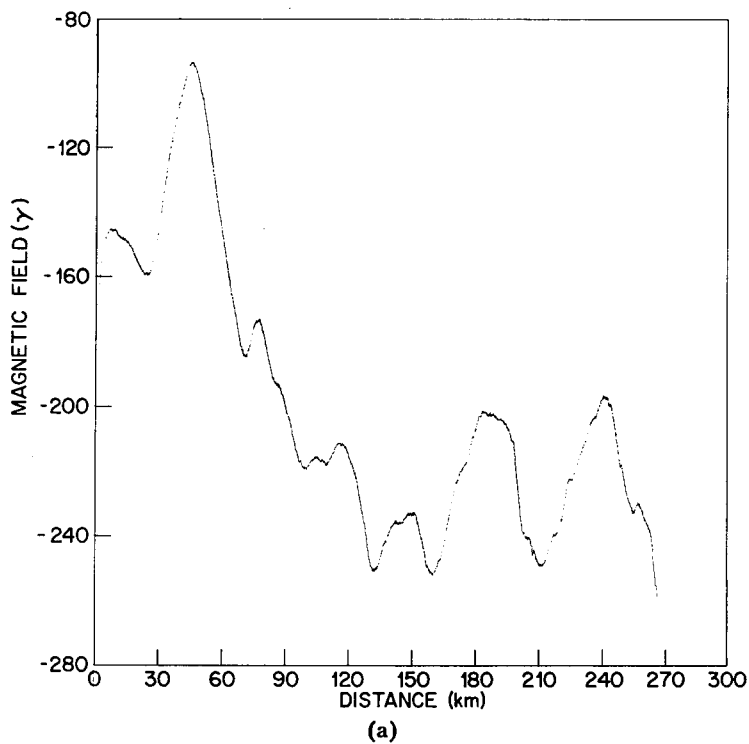


Fig. 5 — Residual fields measured in the Blake area. All distances are measured from west to east, and all have the same scale. (a) Track I, (b) Track II, (c) Track III, (d) Track IV, (e) Track V, (f) Track VI, (g) Track VII, (h) Track VIII, (i) Track IX.

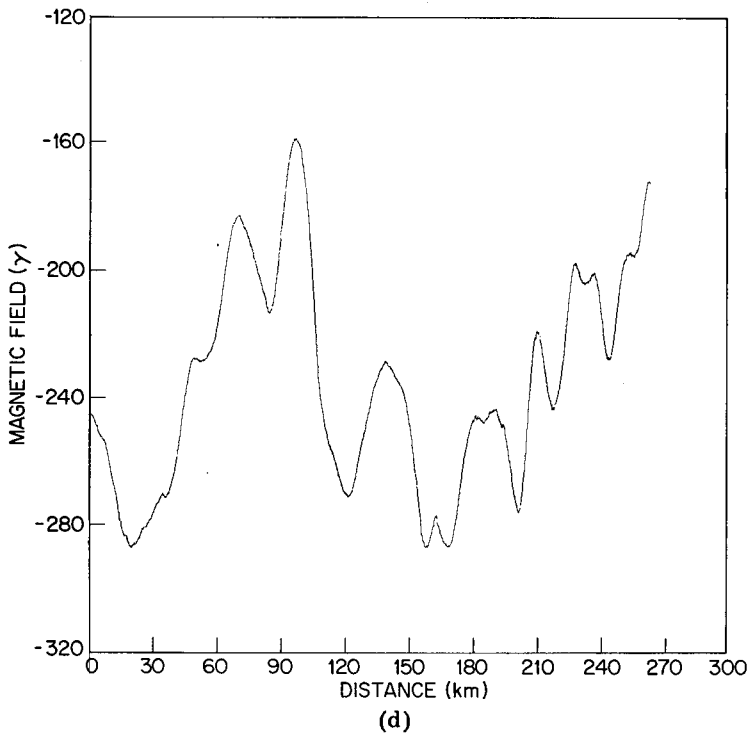
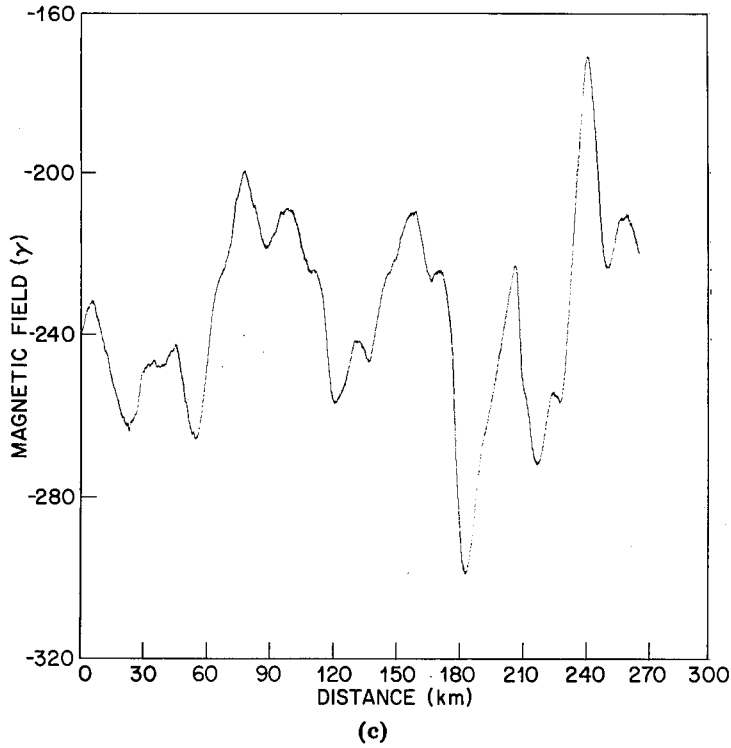
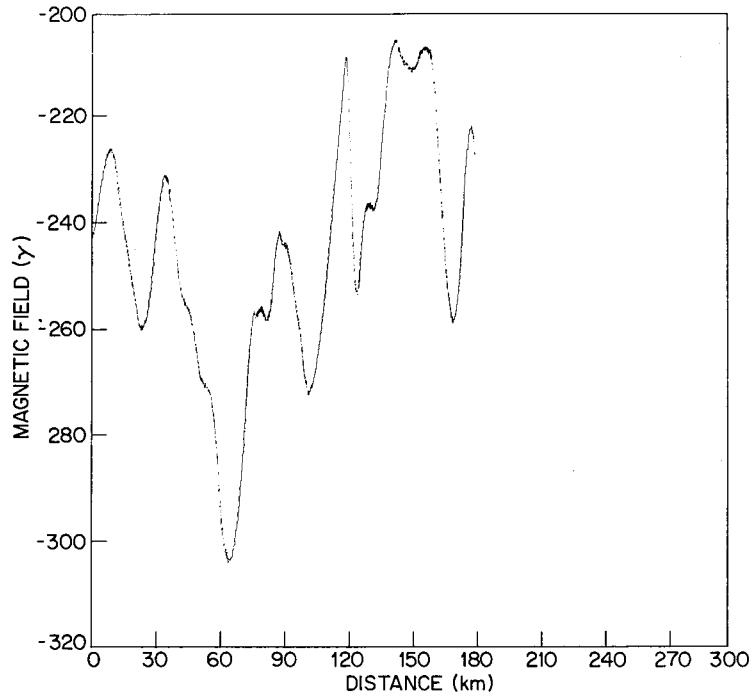
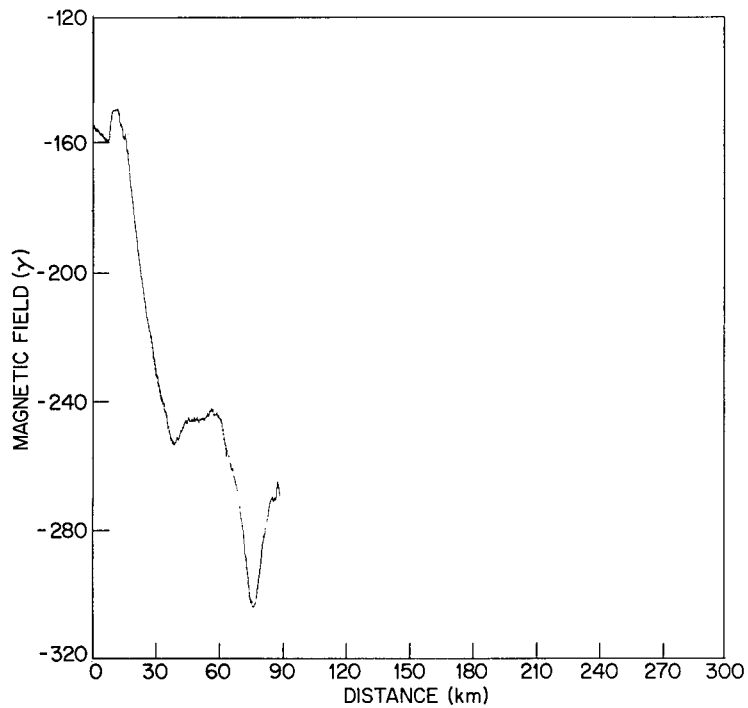


Fig. 5 (continued) — Residual fields measured in the Blake area. All distances are measured from west to east, and all have the same scale. (a) Track I, (b) Track II, (c) Track III, (d) Track IV, (e) Track V, (f) Track VI, (g) Track VII, (h) Track VIII, (i) Track IX.



(e)



(f)

Fig. 5 (continued) — Residual fields measured in the Blake area. All distances are measured from west to east, and all have the same scale. (a) Track I, (b) Track II, (c) Track III, (d) Track IV, (e) Track V, (f) Track VI, (g) Track VII, (h) Track VIII, (i) Track IX.

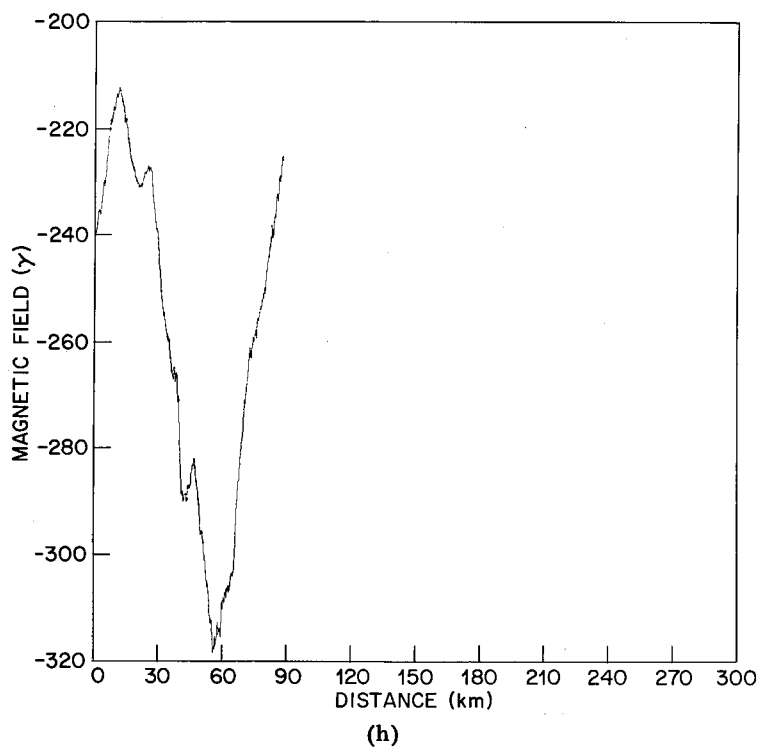
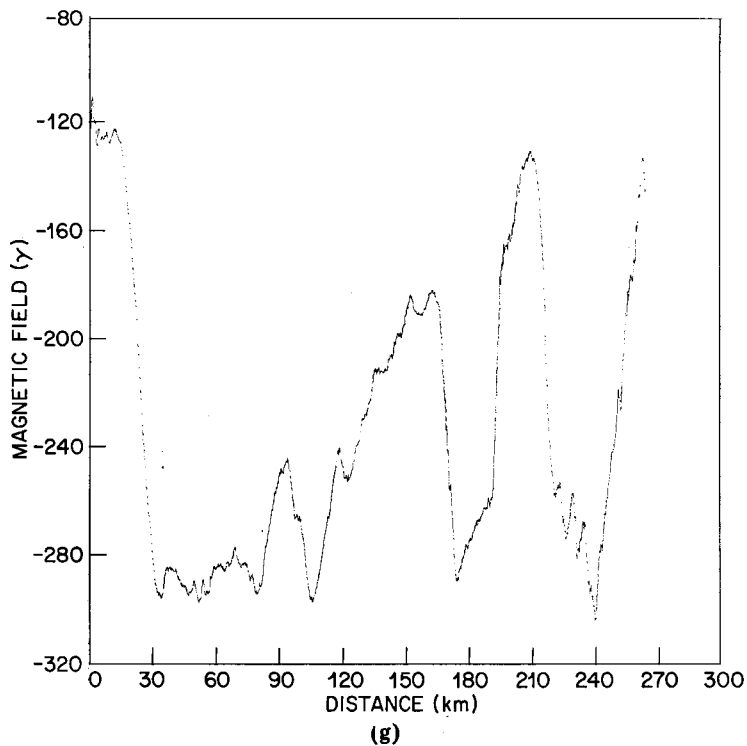


Fig. 5 (continued) — Residual fields measured in the Blake area. All distances are measured from west to east, and all have the same scale. (a) Track I, (b) Track II, (c) Track III, (d) Track IV, (e) Track V, (f) Track IV, (g) Track VII, (h) Track VIII, (i) Track IX.

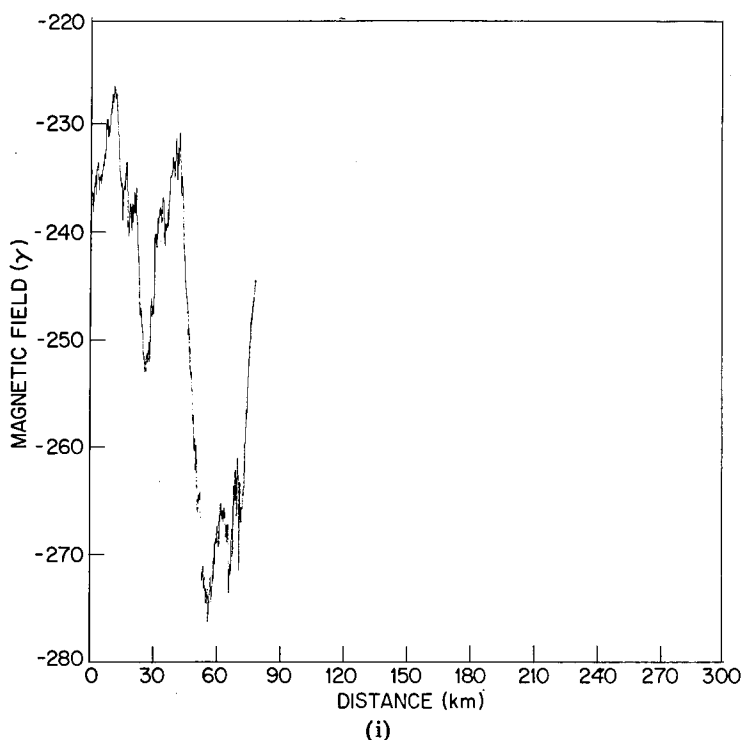
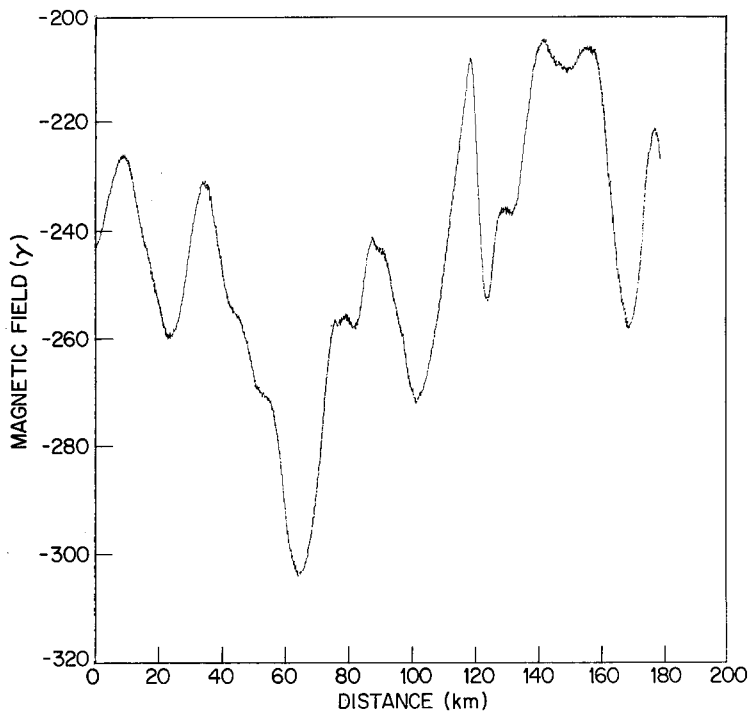


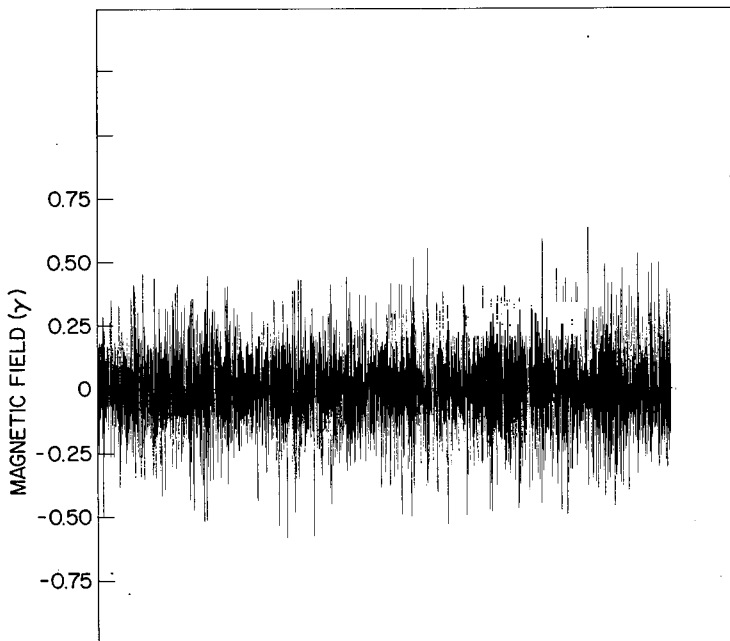
Fig. 5 (continued) — Residual fields measured in the Blake area. All distances are measured from west to east, and all have the same scale. (a) Track I, (b) Track II, (c) Track III, (d) Track IV, (e) Track V, (f) Track VI, (g) Track VII, (h) Track VIII, (i) Track IX.

The sorting histograms for all the Blake tracks are shown in Figs. 8 and 9. It is clear from the N (Γ) results both here and in the Seamounts area that the Quiet Zone is indeed quiet; most of the peaks lie below 40γ , and there is none higher than 80γ . In the more active zones to the east the geological anomalies are similar in width but run two to five times higher in amplitude.

Finally, the geological components of all the Blake tracks are plotted together in Fig. 10 as a function of position. Certain features are common to neighboring tracks, and a trend running north to northeast is faintly discernible. Once again the inability to separate the effects of subbottom topography from magnetization changes prevents us from drawing firm conclusions, but the spacing between the main peaks, 30 to 40 km, is consistent with that observed by Vogt, Anderson, and Bracey [3] in their analysis of the Keathley data, taken in the more active region east and south of this area. We tentatively conclude, therefore, that magnetization patterns and not topography are responsible for the anomalies we have observed. The reason for the low amplitudes remains obscure, but better knowledge of the depth and configuration of the magnetic subbottom would be of obvious value.

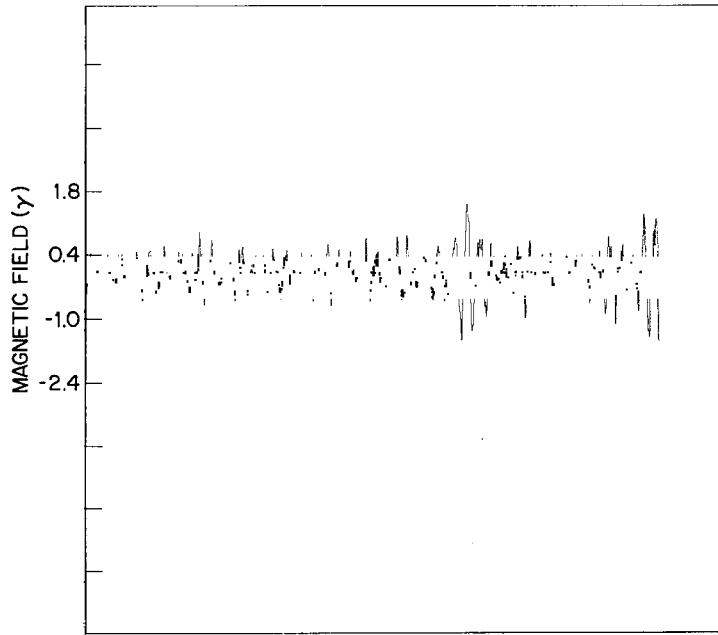


(a)

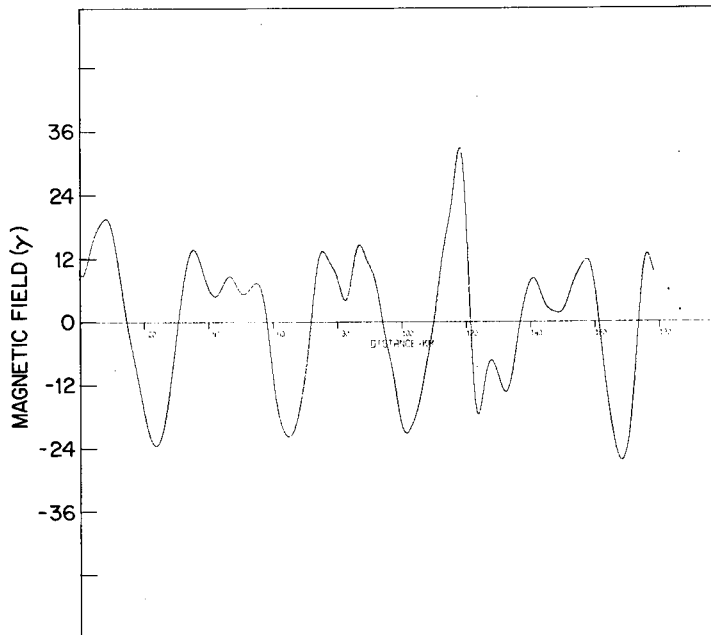


(b)

Fig. 6 — Residual field for track V (characterized by a low level of geomagnetic noise) and its three components after filtering: (a) Residual field, (b) Instrument and wave noise (24 to 120 s), (c) Geomagnetic noise (120 to 1200 s), (d) Geological noise (1200 to 12,000 s) or 5 to 50 km .

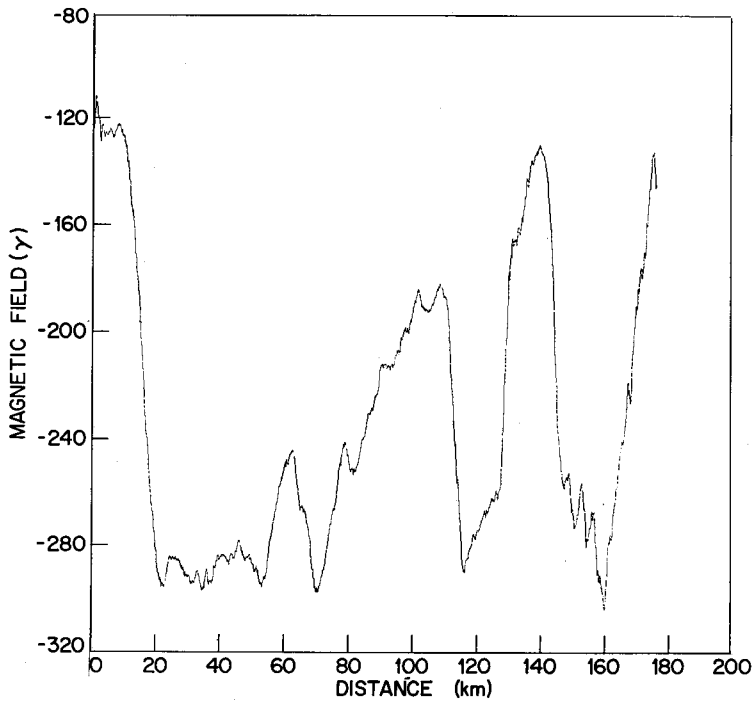


(c)

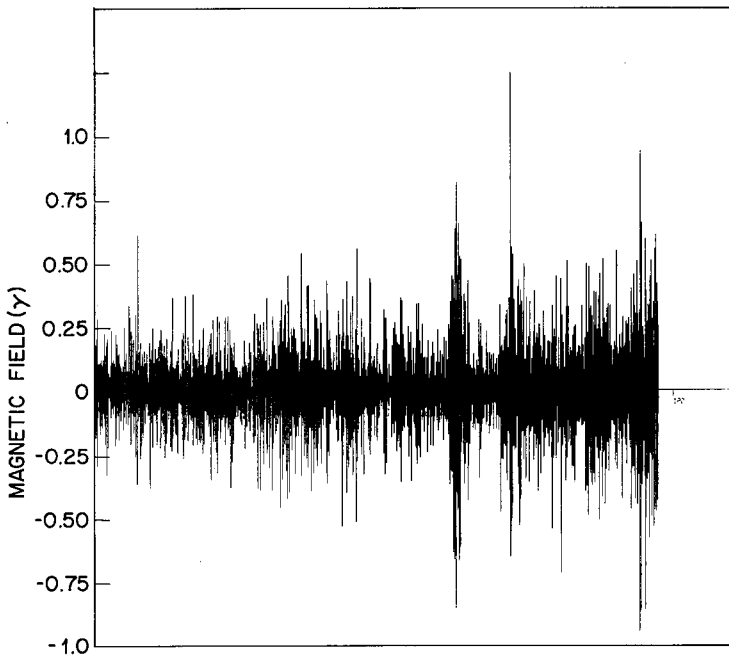


(d)

Fig. 6 (continued) — Residual field for track V (characterized by a low level of geomagnetic noise) and its three components after filtering: (a) Residual field, (b) Instrument and wave noise (24 to 120 s), (c) Geomagnetic noise (120 to 1200 s), (d) Geomagnetic noise (1200 to 12,000 s or 5 to 50 km).

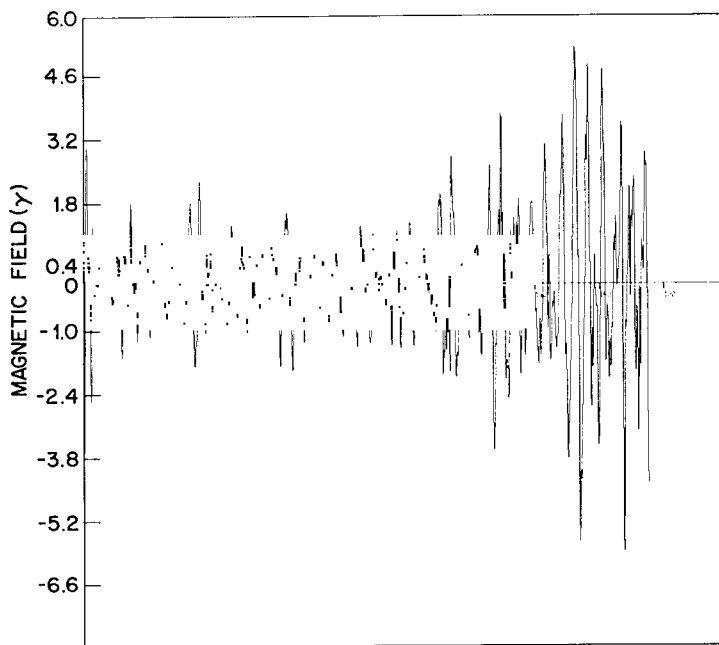


(a)

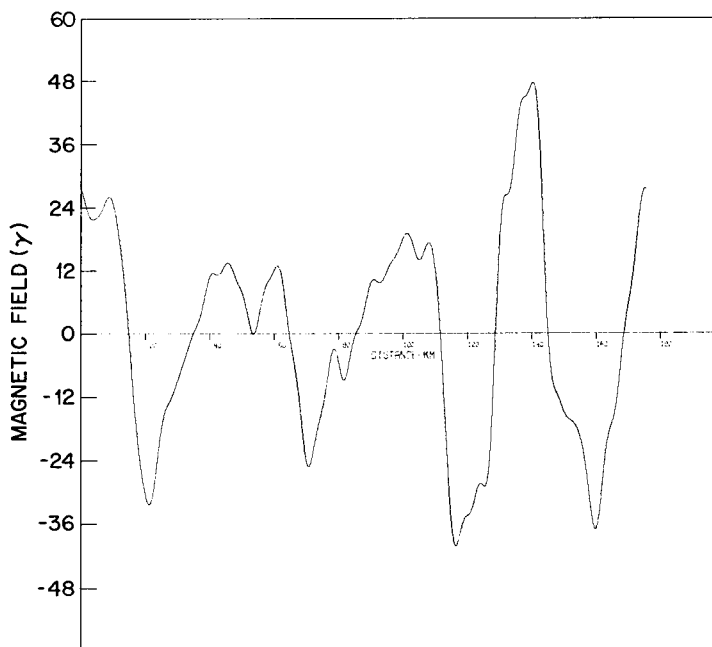


(b)

Fig. 7 -- Residual field for track VII (characterized by a high level of geomagnetic noise) and its three components. (a) Residual field, (b) Instrument and wave noise (24 to 120 s, with some contribution from sharp gradients), (d) Geological noise (120 to 1200 s), (d) Geological noise (120 to 12,000 s or 5 to 50 km.)



(c)



(d)

Fig. 7 (continued) — Residual field for track VII (characterized by a high level of geomagnetic noise) and its three components. (a) Residual field, (b) Instrument and wave noise (24 to 120 s, with some contribution from sharp gradients), (c) Geomagnetic noises (120 to 1200 s), (d) Geological noise (1200 to 12,000 s or 5 to 50 km).

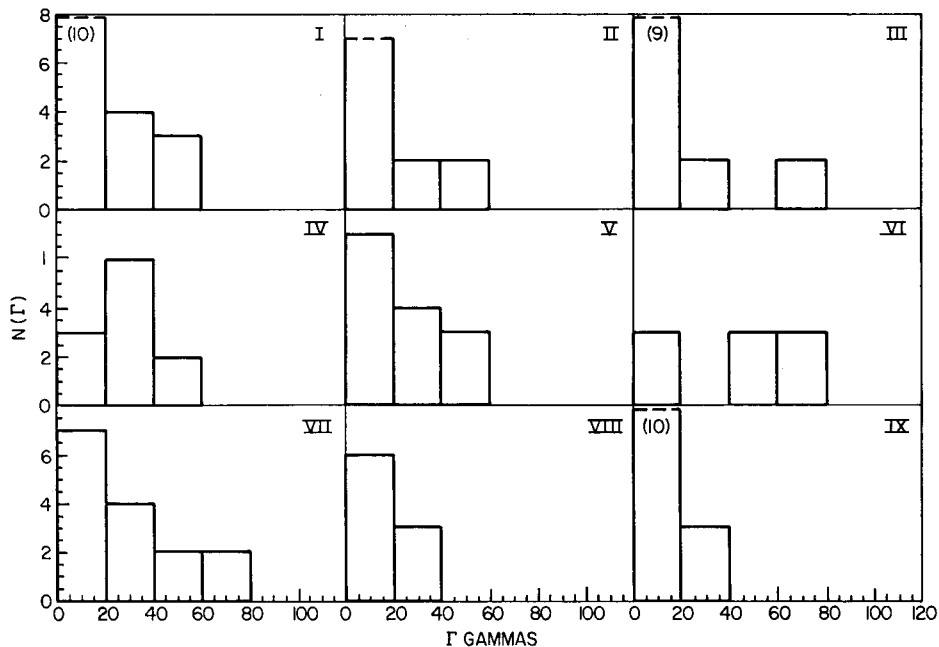


Fig. 8 — Amplitude histograms for the 5-to 50-km filter outputs, Blake tracks. Counts have been scaled to compensate for different lengths of track.

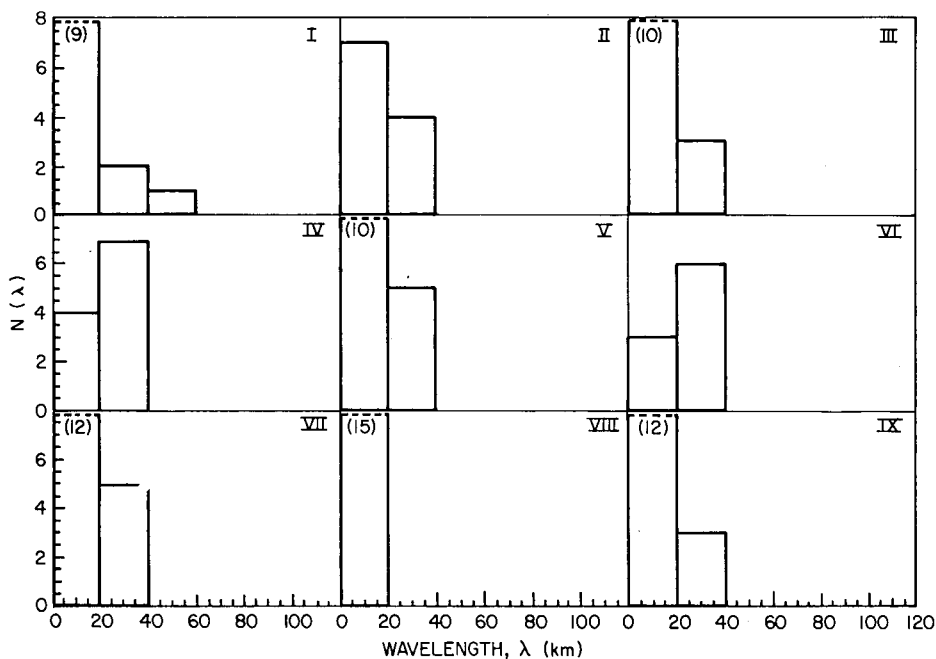


Fig. 9 — Wavelength histograms for the 5-to 50-km filter outputs, Blake tracks. Counts have been scaled to compensate for different lengths of track.

ALERS AND BERGIN

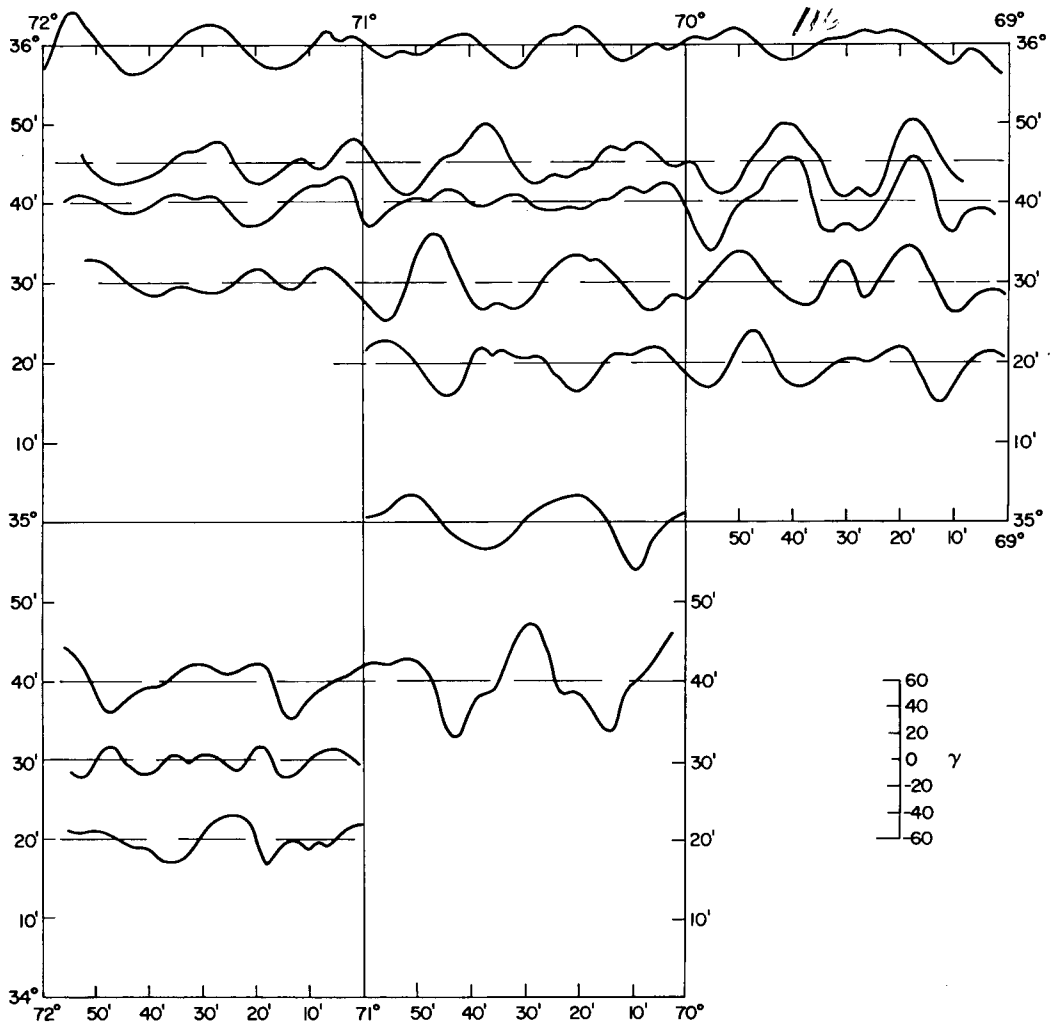


Fig. 10 — Plot of all geologic components of tracks in the Blake area arranged according to relative positions. A scale of field amplitudes is given at lower right. A faint north to northeast trend can be distinguished in the overall pattern.

Geomagnetic Noise

Geomagnetic noise is caused by ionospheric currents that cause perturbations in the earth's field as measured at its surface. All magnetic records gathered on this trip showed varying levels of this type of interference, but VII, VIII, and IX were especially noisy. These data were taken June 10 and 11, 1973; subsequent analysis [4] of observatory records showed that the activity index K_p was of the order of 5. (This activity was associated with the appearance of a spectacular solar flare, photographed by the Skylab crew, now being analyzed by the Space Sciences Division at NRL). Accordingly, the output of the 120-to 1200-s filter for each of these tracks was sorted to yield heights as a function of duration

in time. Figure 11 shows two curves, one derived from a quiet track, track V, and the other from track VII, a noisy record taken 18 hr later. The curve from track V shows a noise spectrum typical of those we encountered on most of our tracks. The peak at 450 s in this curve appears at various points in the others, but in general they form a family whose upper bound does not exceed about 3γ . The curve from track VII, on the other hand, is nearly twice as high; it also shows three peaks that are more or less evenly spaced. Tracks VIII and IX yield similar spectra with the peaks shifted in the direction of longer period.

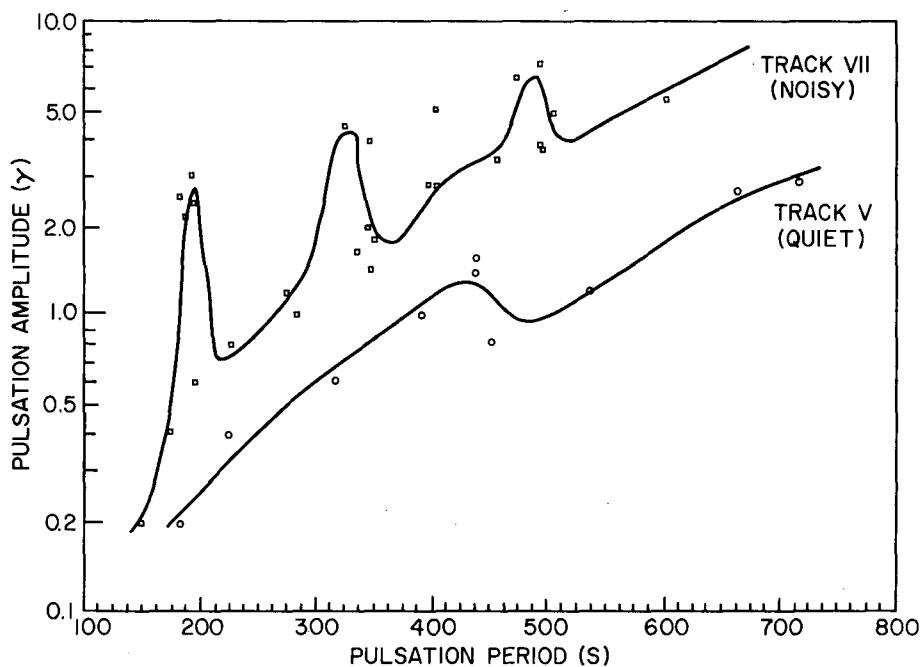


Fig. 11 — Geomagnetic noise spectra for tracks V and VII derived from the output of the 120-to 1200-s filter applied to the residual field traces for these two tracks

Geomagnetic pulsations of this general duration and magnitude have been frequently observed and are classified on the basis of their periodicity as PC4 events (International Union of Geodesy and Geophysics nomenclature). The presence of multiple periods, harmonically related, suggests a standing wave or resonance phenomenon, and most models for the long period PC pulsations are based on the propagation of Alfvén waves excited by bursts of solar activity through the layers of the ionosphere [5].

Whatever the mechanism, it is clear that on days which are even moderately noisy, signals of the order of a gamma in this wavelength/period band will be seriously masked by the background noise, and for certain critical periods, which change rather slowly with time, such signals will be completely obliterated. To meet this problem, consideration should be given to the use of a gradiometer, especially when measurements are to be made

from a slow-moving platform such as a ship. Such an instrument consists of two sensors separated by a fixed distance. Readings are taken simultaneously, and their difference reflects the difference in the geological background field at the two sensor positions; the geomagnetic noise, being the same at both sensors, cancels out. The differences are then integrated with respect to distance along the track, and the result is the geological component.

CONCLUSIONS

Excluding the magnetic signatures of the seamounts themselves, the magnetic environment in the Seamounts area is essentially the same as that of the Blake area to the southwest and can be considered to be part of the Quiet Zone.

The geological magnetic features we observed in the Blake area appear to be part of the same system of lineations observed further east, but with greatly reduced amplitudes. This implies that field reversals were taking place while the Quiet Zone subbottom was being formed. However, information on the bathymetry of the subbottom is lacking, and this conclusion must remain tentative.

Because of instrumental limitations, no geological lineations less than 5 km in width could be resolved. Therefore, all features with periods corresponding to distances of 5 km or less (1200 s or less) were assumed to be entirely the result of geomagnetic disturbances.

Normal geomagnetic background noise was characterized by pulsations or more or less random width with amplitudes in the 0.2- to 3- γ range. On magnetically noisy days, however, the background rose by about a factor of 3, and peaks appeared in the pulse spectrum with amplitudes 2 to 3 γ above this background. This renders detection operations with a single sensor aboard a slow-moving platform almost impossible. However, gradiometric techniques involving a pair of sensors can greatly reduce the effects of such interference.

SUGGESTIONS FOR FUTURE WORK

Further efforts should be made to establish the location and features of the magnetic subbottom in the Quiet Zone. Such information, when coordinated with magnetic measurements, would allow us to separate magnetic effects from topographic variations. It would also help to determine whether the magnetic subbottom is significantly deeper or thinner or of different composition in the Quiet Zone than elsewhere. These possibilities have all been suggested as explanations for the low level of magnetic activity observed.

Magnetic measurements should be taken at sea with a gradiometer to determine its advantages and drawbacks in actual operation. To compensate for the relatively low sensitivity of the resonance sensors, a long baseline (200 m) should be used. This is quiet feasible for a ship; it is less so for aircraft. The expected sensitivity of 1×10^{-3} is an order of magnitude less than what is projected for the new superconducting gradiometer, but this instrument is still in the early stages of development. The quality of data obtainable with

the resonance device should provide valuable guidelines for decisions yet to be made in the evolution of the superconducting instrument. At the same time, the ability of the gradiometer to separate geomagnetic noise from magnetic geology should be of considerable value in both magnetic surveying and detection problems.

ACKNOWLEDGMENTS

The authors wish to thank John L. Gregson, III, of the Ocean Sciences Division for his technical help in the operation of the magnetometer and data acquisition equipment and Ralph Gallatin and Guy Mullis of the Ship Facility Group for their supervision of the ship-board mechanical and electronic equipment used during the trip. Jack Ostrander, also of the Ship Facility Group, prepared the special loran-c charts, L. P. LaLumiere of the Acoustics Division provided the International Geomagnetic Reference Field routine, and the land-based magnetic data from the Fredericksburg Observatory were obtained from the World Data Center-A for Solar-Terrestrial Physics, National Oceanic and Atmospheric Administration, Boulder, Colorado. The Master, officers, and crew of the USNS *Mizar* were, as always, unfailingly courteous and helpful throughout the trip.

REFERENCES

1. P.B. Alers, J.M. Bergin, and D. Greenwalt, "Surface and Bottom Magnetic Survey in the Area of the Bermuda Rise," NRL Report 7645, 1973.
2. E. Uchupi, J.D. Phillips and K.E. Prada, "Origin and Structure of the New England Seamount Chain," *Deep Sea Res.* 17, 483 (1970).
3. P.R. Vogt, C.N. Anderson, and D.R. Bracey, "Mesozoic Magnetic Anomalies, Sea-Floor Spreading, and Geomagnetic Reversals in the Southwestern North Atlantic," *J. Geophys. Res.* 76, 4796 (1971).
4. J.V. Lincoln, editor, "Geomagnetic and Solar Data," *J. Geophys. Res.* 78, 6832 (1973).
5. W.H. Campbell, "Geomagnetic Pulsations," in *Physics of Geomagnetic Phenomena* (S. Matsushita and W.H. Campbell, editors), Vol. II, Chap. IV-4, Academic Press, New York and London, 1967.

